Numerical and Analytical Solutions for Ovaling Deformation in Circular Tunnels Under Seismic Loading

Ahmad Fahimifar[1], Arash Vakilzadeh[2]
[1] Department of Civil and Environmental Engineering, Amirkabir University of Technology, Tehran, Iran
Email: fahim@aut.ac.ir
[2] Department of Civil and Environmental Engineering, Amirkabir University of Technology, Tehran, Iran
Email: vakilzadeh.arash@gmail.com

***Abstract*: Ovaling deformations develop when waves propagate perpendicular to the tunnel axis. Two analytical solutions are used for estimating the ovaling deformations and forces in circular tunnels due to soil–structure interaction under seismic loading. In this paper, these two closed form solutions will be described briefly, and then a comparison between these methods will be made by changing the ground parameters. Differences between the results of these two methods in calculating the magnitudes of thrust on tunnel lining are significant. For verifying the results of these two closed form solutions, numerical analyses were performed using finite element code (ABAQUS program). These analyses show that the two closed form solutions provide the same results only for full-slip condition.**

***Key words*: Seismic analyses, ovaling deformation, circular tunnel, soil-structure**

I. Introduction

Ovaling deformation is the most significant influence on the tunnel lining under seismic loading, except for the case of the tunnel being directly sheared by a fault (Penzien, 2000). Ovaling deformations develop when waves propagate perpendicular to the tunnel axis and are therefore, designed for in the transverse direction (typically under two-dimensional, plane-strain conditions). Studies have suggested that, while ovaling may be caused by waves propagating horizontally or obliquely, vertically propagating shear waves are the predominant form of earthquake loading that causes these types of deformations [1].

II. A Review on the Ovaling Deformations of Circular Tunnels

A. Ovaling Deformations of Circular Tunnels Without Soil-Structure Interaction

The simplest form of estimating ovaling deformation is to assume the deformations in a circular tunnel to be identical to ''free-field'', thereby ignoring the tunnel–ground interaction. This assumption is appropriate when the ovaling stiffness of the lined tunnel is equal to that of the surrounding ground. Ground shear distortions can be defined in two ways, as shown in Fig. 1. In the non-perforated ground, the maximum diametric strain is a function of maximum free-field shear strain only deformations [2].

$$\frac{\Delta d}{d} = \pm \frac{\gamma_{\max}}{2} \qquad (1)$$

The diametric strain in a perforated ground is further related to the Poisson's ratio of the medium [2].

$$\frac{\Delta d}{d} = \pm 2\gamma_{\max}(1-\vartheta_m) \qquad (2)$$

Where $\gamma_{\max}$ is the maximum free-field shear strain of soil or rock medium, ϑ_m is the Poisson's ratio of the medium and d is the diameter of tunnel lining. Both of these equations assume the absence of the lining, therefore ignoring tunnel-ground interaction. In the free-field, the perforated ground would yield a much greater distortion than the non-perforated, sometimes by a factor of two or three. This provides a reasonable distortion criterion for a lining with little stiffness relative to the surrounding soil, while the non-perforated deformation equation will be appropriate when the lining stiffness is equal to that of the medium. A lining with large relative stiffness should experience distortions even less than those given by (1), [1].

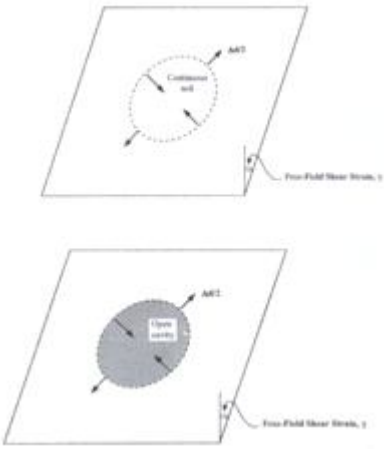

Fig 1. Free-field shear distortion of perforated and non-perforated ground, circular shape(after Wang, 1993

DOI: 01.IJTUD.01.02.353

B. Ovaling Deformations of Circular Tunnels With Soil-Structure Interaction

In most cases the lining ground interaction has to be taken into account. As a first step, the relative stiffness of the tunnel to the ground is quantified by the compressibility and flexibility ratios (C and F), which are measures of the extensional and flexural stiffnesses (resistance to ovaling), respectively, of the medium relative to the lining [3], [4].

$$C = \frac{E_m(1-\vartheta_l^2)r}{E_l t(1+\vartheta_m)(1-2\vartheta_m)} \quad (3)$$

$$F = \frac{E_m(1-\vartheta_l^2)r^3}{6E_l I(1+\vartheta_m)} \quad (4)$$

Where E_m is the modulus of elasticity of the medium, I is the moment of inertia of the tunnel lining (per unit width) for circular lining, ϑ_l is the Poisson's ratio of tunnel lining, E_l is the modulus of elasticity of the tunnel lining, r and t the radius and thickness of the tunnel lining, respectively. In early studies of racking deformations, Peck et al. (1972), based on earlier work by Burns and Richard (1964) and Hoeg (1968), proposed closed-form solutions in terms of thrusts, bending moments, and displacements under external loading conditions. The response of a tunnel lining is expressed as functions of the compressibility and flexibility ratios of the structure, and the in-situ overburden pressure and at-rest coefficient of earth pressure of the soil.

The solutions are developed for both full-slip and no-slip condition between the tunnel and the lining. Full-slip condition results in no tangential shear force [2]. Wang (1993) reformulated the equations to adapt to seismic loadings caused by shear waves. The free-field shear stress replaces the in situ overburden pressure and the at-rest coefficient of earth pressure is assigned a value of (-1) to simulate simple shear condition. The shear stress is expressed as a function of shear strain:

$$\tau = G\gamma_m \quad (5)$$

$$\gamma_m = \frac{V_s}{C_s} \quad (6)$$

Where τ is the simple shear stress of soil element , G is the shear modulus of soil or rock medium, γ_m is the maximum shear strain, V_s peak particle velocity associated with S-waves, C_s is the apparent velocity of S-wave propagation. Assuming full-slip conditions, without normal separation and therefore, no tangential shear force, the diametric strain, the maximum thrust, and bending moment can be expressed as (Wang, 1993):

$$\frac{\Delta d}{d} = \pm\frac{1}{3}K_1 F\gamma_{\max} \quad (7)$$

$$T_{\max} = \pm\frac{1}{6}K_1\frac{E_m}{1+\vartheta_m}r\gamma_{\max} \quad (8)$$

$$M_{\max} = \pm\frac{1}{6}K_1\frac{E_m}{1+\vartheta_m}r^2\gamma_{\max} \quad (9)$$

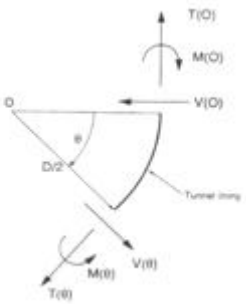

Fig 2. Sign convention for force components in circular lining (after Penzien, 2000).

$$K_1 = \frac{12(1-\vartheta_m)}{2F+5-6\vartheta_m} \quad (10)$$

These forces and moments are illustrated in Fig. 2.

According to various studies, slip at the interface is only possible for tunnels in soft soils or cases of severe seismic loading intensity. For most tunnels, the interface condition is between full-slip and no-slip, so both cases should be investigated for critical lining forces and deformations. However, full-slip assumptions under simple shear may cause significant underestimation of the maximum thrust, so it has been recommended that the no-slip assumption of complete soil continuity be made in assessing the lining thrust response [3],[5].

$$T_{\max} = \pm K_2\tau_{\max}r = \pm K_2\frac{E_m}{2(1+\vartheta_m)}r\gamma_{\max} \quad (11)$$

$$K_2 = 1 + \frac{F\left[(1-2\vartheta_m)-(1-2\vartheta_m)C\right]-\frac{1}{2}(1-2\vartheta_m)^2+2}{F\left[(3-2\vartheta_m)+(1-2\vartheta_m)C\right]+C\left[\frac{5}{2}-8\vartheta_m+6\vartheta_m{}^2\right]+6-8\vartheta_m} \quad (12)$$

Where $\tau_{\max}$ is the maximum shear stress.

Note that no solution is developed for calculating diametric strain and maximum moment under no-slip condition. It is recommended that the solutions for full-slip condition be used for no-slip condition. The more conservative estimates of the full-slip condition is considered to offset the potential underestimation due to pseudo-static representation of the dynamic problem [1].

According to (13) and Fig. 3, a tunnel lining will deform less than the free field when the flexibility ratio is less than one (i.e. stiff lining in soft soil). As the flexibility ratio increases, the lining deflects more than the free field and may reach an upper limit equal to the perforated ground deformations. This condition continues as the flexibility ratio becomes infinitely large (i.e. perfectly flexible lining).

$$\frac{\Delta d_{lining}}{\Delta d_{free-field}} = \frac{2}{3}K_1 F \quad (13)$$

DOI: 01.IJTUD.01.02.353

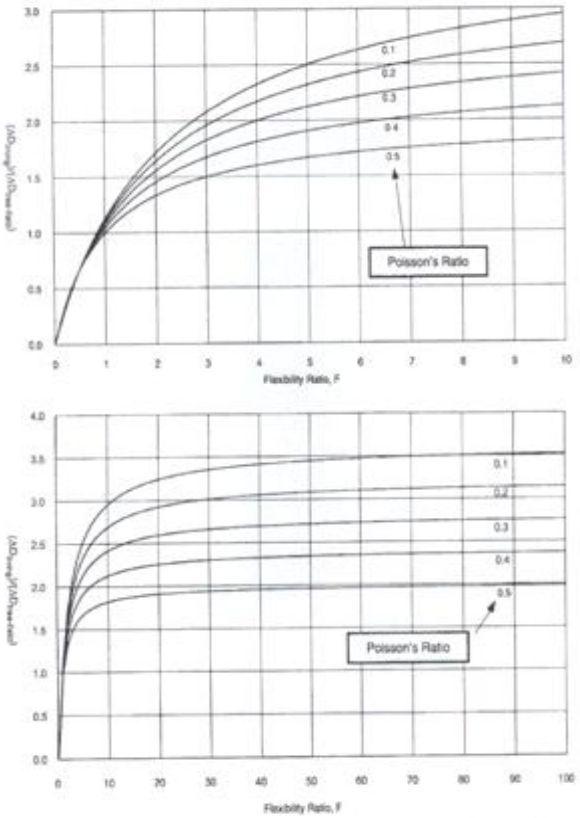

Fig 3. Normalized lining deflection vs. flexibility ratio, full slip interface, and circular lining (Wang, 1993).

Ref. [8], [6] developed similar analytical solutions for maximum thrust, shear, and moment in the tunnel lining due to ovaling deformations. Assuming full slip condition, solutions for thrust, moment, and shear in circular tunnel linings caused by soil–structure interaction during a seismic event are expressed as [6].

$$\Delta d^{n}{}_{lining} = R^{n}\Delta d_{free-field} = R^{n}\frac{d}{2}\gamma_{\max} \qquad (14)$$

$$T_{\max} = \pm\frac{12E_{l}I\Delta d^{n}{}_{lining}}{d^{3}(1-\upsilon_{l}^{2})} \qquad (15)$$

$$M_{\max} = \pm\frac{6E_{l}I\Delta d^{n}{}_{lining}}{d^{2}(1-\upsilon_{l}^{2})} \qquad (16)$$

$$V_{\max} = \pm\frac{24E_{l}I\Delta d^{n}{}_{lining}}{d^{3}(1-\upsilon_{l}^{2})} \qquad (17)$$

The lining-soil racking ratio under normal loading only is defined as:

$$R^{n} = \pm\frac{4(1-\upsilon_{m})}{(\alpha^{n}+1)} \qquad (18)$$

$$\alpha^{n} = \frac{12E_{l}I(5-6\upsilon_{m})}{d^{3}G_{m}(1-\upsilon_{l}^{2})} \qquad (19)$$

In the case of no slip condition, the formulations are presented as:

$$\Delta d_{lining} = R\Delta d_{free-field} = R\frac{d}{2}\gamma_{\max} \qquad (20)$$

$$T_{\max} = \pm\frac{24E_{l}I\Delta d_{lining}}{d^{3}(1-\upsilon_{l}^{2})} \qquad (21)$$

$$M_{\max} = \pm\frac{6E_{l}I\Delta d_{lining}}{d^{2}(1-\upsilon_{l}^{2})} \qquad (22)$$

$$V_{\max} = \pm\frac{24E_{l}I\Delta d_{lining}}{d^{3}(1-\upsilon_{l}^{2})} \qquad (23)$$

Where:

$$R = \pm\frac{4(1-\upsilon_{m})}{(\alpha+1)} \qquad (24)$$

$$\alpha = \frac{24E_{l}I(3-4\upsilon_{m})}{d^{3}G_{m}(1-\upsilon_{l}^{2})} \qquad (25)$$

Where $T_{\max}$, $M_{\max}$ and $V_{\max}$ are the maximum thrust, maximum bending moment and maximum shear force in tunnel cross-section due to shear waves, respectively. $\Delta d^{n}{}_{lining}$ is the lining diametric deflection under normal loading only, R^{n} is the lining-soil racking ratio under normal loading only, Δd_{lining} is the lining diametric deflection, R is the lining-soil racking ratio and $\Delta d_{free-field}$ is free-field diametric deflection in non-perforated ground.

Ref. [2] compared Wang (1993) and Penzien (2000) closed form solutions. They concluded that magnitude of the thrust on tunnel lining in Wang solutions provides a higher estimate than Penzien solutions for no-slip condition. In another paper [7], they performed a series of numerical analyses using the finite element code Plaxis to evaluate these analytical solutions.

In this paper, a comparison with numerical analyses demonstrated that the maximum thrust in the tunnel lining of the Wang solution for the no-slip condition provides a higher estimate than Penzien again and also the magnitude of the thrust in Wang solutions provides a realistic estimate for no-slip condition. He recommended that Penzien's solutions not be used for no-slip condition. It was also showed that the calculated forces and displacements are identical for the condition of full-slip between the tunnel and the ground, for both Wang and Penzien solutions.

A series of analyses were performed by the authors in this paper, reveal that magnitude of the maximum thrust for no-slip condition is much higher than the maximum thrust for full-slip condition, even with increasing flexibility ratio does not decrease in comparison to the maximum thrust forces in full-slip condition. For this reason, a comparison has been

DOI: 01.IJTUD.01.02. 353

made between K_1 and K_2 introducing full-slip lining response coefficient and no-slip lining response coefficient, respectively (Fig. 4).

As is observed decreases considerably as the flexibility ratio increases. By approaching the flexibility ratio to 80, tends to zero. As (8) shows, the maximum thrust () is directly proportional to the ,therefore, by increasing flexibility ratio, maximum thrust in the tunnel lining decreases in full-slip condition, however, the maximum thrust is not change, actually. However the changes of by increasing the flexibility ratio is not considerably, as the result, maximum thrust in no-slip condition dose not approach to zero and even sometimes increases by increasing the flexibility ratio.

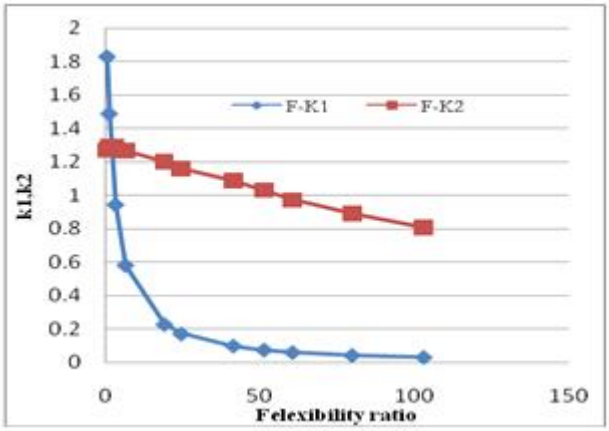

Fig 4. Comparison of K_1 and K_2 vs. flexibility ratio

III. Numerical Analyses for Comparing the Closed Form Solutions

Eleven numerical analyses were performed using the finite element method ABAQUS to compute and evaluate the analytical solutions for ovaling deformations of circular tunnels. In these analyses the following assumptions were made which are the same as assumptions made by Wang and Penzien : (a) plane strain condition (b) ground and lining are linear elastic and homogenous , (c) shear loading is applied at the upper ends of the boundaries to simulate pure shear conditions.

In ABAQUS, only no-slip condition between the tunnel lining and ground is simulated. The numerical analysis is first verified by analyzing non-perforated and perforated ground. The computed ovaling deformations are nearly identical to those obtained from (1) and (2). In these analyses the dimensions and material properties of the lined tunnel are:

Lining thickness (t): 0.3m, moment of inertia (I): $0.00225\,{}^{m^4}\!/_{m}$, Area (per unit width): $0.3\,{}^{m^2}\!/_{m}$, lining diameter: 6m,

E_l = 24,800,000 ${}^{KN}\!/_{m^2}$ and

thickness of the overburden= 15m

Earthquake and ground parameters:

Young'smodulus(E_m):10000-2,000,000, =5000-667111 , =0.012-0.0011, =0-0.499, =1.92 and =0.63

The result of these analyses were compared and summarized as follows:

1) As discussed above, and according to Fig. 5 numerical analyses results agree with Wang's maximum thrust in no-slip condition, when the flexibility ratio increases. Fig. (5) also Shows that the curve belonging to Wang' solutions can be converted to the curve belonging to the numerical analysis by multiplying 1.15 to the Wang's closed form solutions. This figure also reveals that Penzien's solution underestimates significantly the magnitude of thrust in tunnel lining for the condition of no-slip.

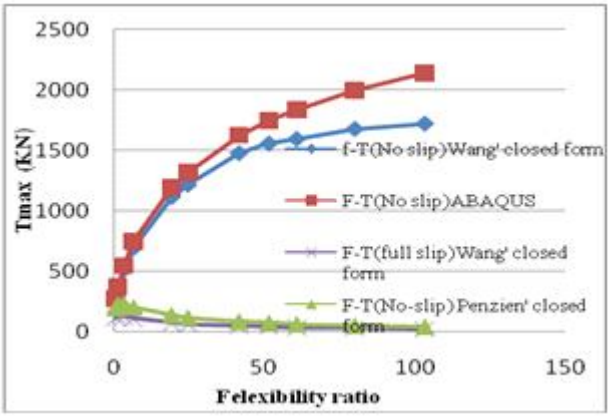

Fig 5. Comparison of T_{max} of closed form solutions and numerical analyses vs. flexibility ratio

2) Fig. 6 indicates that increase in flexibility ratio, the maximum bending moment decreases for both numerical analyses and Penzien's solutions in no-slip condition and for Wang's solutions in full-slip condition. Ref. [1] recommended to use full-slip condition for maximum bending moment in seismic design of tunnels. Here, for $F \prec 50$ it can be observed again as in Fig. 6, that Wang's maximum bending moment in full-slip condition is higher than the result of numerical analyses, while for $F \succ 50$ the maximum bending moment in numerical analyses become just a little higher than the Wang's maximum bending moment in full-slip condition. It should be mentioned that this trend is exactly repeated for Penzien's maximum bending moment in no-slip condition. The result of Wang's and Penzien's maximum bending moment in full-slip condition are identically the same.

DOI: 01.IJTUD.01.02. 353

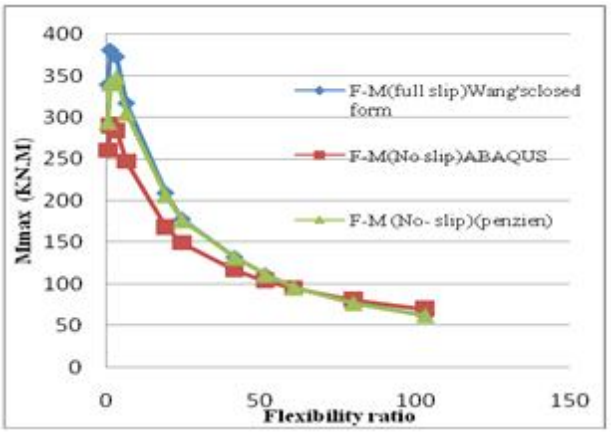

Fig 6. Comparison of M_{max} of closed form solutions and numerical analyses vs. flexibility ratio

3) In Fig. (7) a comparison has been made for normalized deformations in tunnel lining relative to the ground. As it is expected for $F \prec 50$ the results of Wang's solutions in full-slip condition provide higher estimate than numerical analyses in no-slip condition but for $F \succ 50$ result of numerical analyses provide higher estimate than Wang's solutions. The result of Wang's and Penzien's closed form solutions in full-slip condition are identically the same. Penzien's normalized deformations in tunnel lining in full-slip and no-slip condition are almost the same.

4) By increasing the velocity of S-wave propagation, trends of increasing the maximum thrust forces in numerical analyses for no-slip condition provides higher estimate than Wang's maximum thrust in no-slip, full-slip condition and the Penzien's maximum thrust in no-slip condition. The Wang's maximum thrust in full-slip condition and also the Penzien's maximum thrust decreases, as the velocity of S-wave propagation increases Fig. (8).

The trend of decreasing the maximum bending moment for numerical analyses in no-slip condition, Wang's closed form in full-slip and Penzien's closed form in no-slip conditions vs. velocity of S-wave propagation can be observed in Fig. (9).

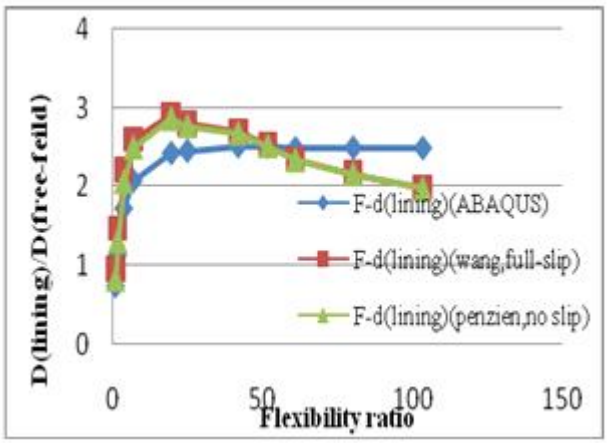

Fig 7. Comparison of normalized deformations in tunnel lining to the ground of closed form solutions and numerical analyses vs. flexibility ratio

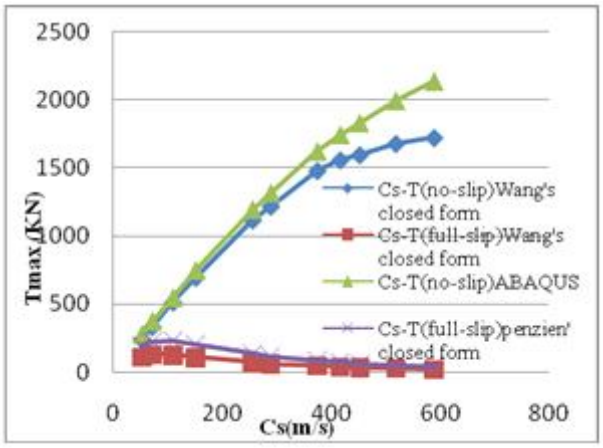

Fig 8. Effect of velocity of S-wave propagation on T_{max} of closed form solutions and numerical analyses

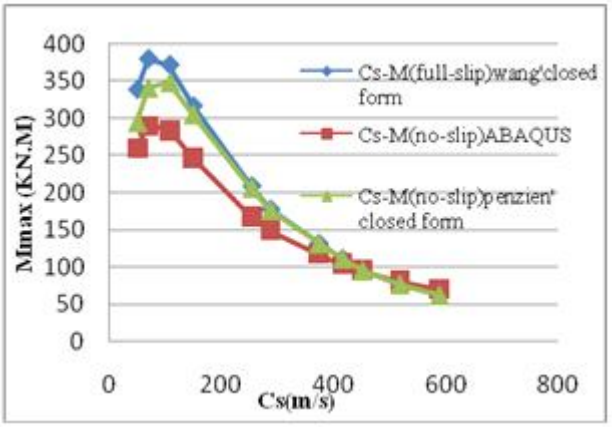

Fig 9. Effect of velocity of S-wave propagation on M_{max} of closed form solutions and numerical analyses

Conclusions

Two analytical Wang's and Penzien' solutions for estimating the ovaling deformation and forces in circular tunnels due to soil–structure interaction under seismic loading are compared and evaluated to numerical analyses ABAQUS. By multiplying 1.15 to the Wang's maximum thrust solutions in no-slip condition provide the realistic result for this condition. Contrary to expect, for $F \succ 50$ the maximum bending moment and normalized deformations in tunnel lining in full-slip condition do not provide higher estimates than no-slip condition. Wang's and Penzien's maximum bending moments and deformations of tunnel are identical for full-slip condition.

Penzien's deformations of tunnel are almost identical for full-slip and no-slip conditions. Finally the maximum thrust and bending moment in full-slip and no-slip conditions are compared to the numerical analyses in no-slip condition by increasing the velocity of S-wave propagation. In these comparisons, the thrust forces in numerical analyses and Wang's closed form in no-slip condition increases by increasing the velocity of S-wave propagation, while the

DOI: 01.IJTUD.01.02. 353

Wang's maximum thrust in full-slip condition and Penzien's maximum thrust in no-slip condition, decreases. With increasing the velocity of S-wave propagation, the Maximum bending moment in numerical and analytical analyses increases for $F \prec 1.0$ and decreases for $F \succ 1.0$.

References

[1] Wang, J.N., 1993. Seismic Design of Tunnels: A State-of-the-art Approach. Parsons Brinckerhoff Quade & Douglas, Inc., New York, NY, Monograph 7.

[2] Hashash, Y.M.A., Hook, J.J., Schmidt, B., Yao, J.I.-C., 2001. Seismic design and analysis of underground structure. Tunn. Undergr. Sp.Technol. 16, 247–293.

[3] Hoeg, K., 1968. Stresses against underground structural cylinders. J.Soil Mech. Found. Div. 94 (SM4).

[4] Peck, R.B., Hendron, A.J., Mohraz, B., 1972. State of the art in soft ground tunneling. In: The Proceedings of the Rapid Excavation and Tunneling Conference. American Institute of Mining, Metallurgical, and Petroleum Engineers, New York, NY, pp. 259–286

[5] Schwartz, C.W., Einstein, H.H., 1980. Improved design of tunnel supports: vol. 1. Simplified analysis for ground structure interaction in tunneling. Report no. UMTA-MA-06-0100-80-4. US DOT, Urban Mass Transportation Administration.

[6] Penzien, J., 2000. Seismically -induced racking of tunnel linings. Int.J. Earthquake Eng. Struct. Dyn. 29, 683_691.

[7] Hashash, Y.M.A., Park, D., Yao, J.I.C., 2005. Ovaling deformations of circular tunnels under seismic loading: an update on seismic design and analysis of underground structures. Tunn. Undergr. Space Technol. 20, 435–441.

[8] Penzien, J., Wu, C.L., 1998. Stresses in linings of bored tunnels. Int. J.Earthquake Eng. Struct. Dynamics 27, 283–300.

DOI: 01.IJTUD.01.02.353